The Astrophysical Journal, 667:351–357, 2007 September 20

GRB 060218: A RELATIVISTIC SUPERNOVA SHOCK BREAKOUT

E. Waxman,[1] P. Mészáros,[2] and S. Campana[3]

Received 2007 February 16; accepted 2007 June 4

ABSTRACT

We show that the prompt and afterglow X-ray emission of GRB 060218, as well as its early ($t \lesssim 1$ day) optical-UV emission, can be explained by a model in which a radiation-mediated shock propagates outward from a compact progenitor star into a dense wind. The prompt thermal X-ray emission is produced in this model when the mildly relativistic shock, $\beta \approx 0.85$, carrying a few times 10^{49} erg, reaches the wind (Thomson) photosphere, where the post-shock thermal radiation is released and the shock becomes collisionless. Adopting this interpretation of the thermal X-ray emission, we predict a subsequent X-ray afterglow, due to synchrotron emission and inverse Compton scattering of supernova UV photons by electrons accelerated in the collisionless shock. Early optical-UV emission is also predicted, due to the cooling of the outer $\delta M \sim 10^{-3}\, M_\odot$ envelope of the star, which was heated to high temperature during the shock passage. The observed X-ray afterglow and the early optical-UV emission are both consistent with those expected in this model. Detailed analysis of the early optical-UV emission may provide detailed constraints on the density distribution near the stellar surface.

Subject headings: gamma rays: bursts — shock waves — supernovae: general

Online material: color figure

1. INTRODUCTION

In our previous paper (Campana et al. 2006), the points mentioned in the Abstract were outlined only briefly, using order-of-magnitude arguments and with very little explanation, due to space limitations. Here we present a more detailed explanation and analysis of the prompt thermal X-ray emission and X-ray afterglow, as well as a calculation of the early optical-UV emission, and show that some claims made in recent publications (Ghisellini et al. 2007; Fan et al. 2006b; Li 2007), according to which the observations are inconsistent with the massive wind interpretation, are not valid.

GRB 060218 was unique mainly in two respects: it showed a strong thermal X-ray emission accompanying the prompt non-thermal emission, and it had a strong optical-UV emission at early, $t \lesssim 1$ day, times. We show here that these features, as well as the X-ray afterglow, can all be explained by a model in which a radiation-mediated shock propagates outward from a compact progenitor star into a massive wind. We have shown in a separate paper (Wang et al. 2007) that the prompt nonthermal X-ray emission can also be explained by this model.

As detailed below, the prompt thermal X-ray emission can be explained as a shock breakout at a radius of $\sim 5 \times 10^{12}$ cm, which requires a Thomson optical depth (of the plasma ahead of the shock) of $\tau \approx 1$. Breakout may occur at $\sim 5 \times 10^{12}$ cm if this is the stellar progenitor radius. However, since the progenitor is likely to be smaller, we suggested the possibility of it being surrounded by an optically thick wind. Another possibility is a pre-explosion ejection of a shell with a small mass, $\sim 10^{-6}\, M_\odot$. Here we adopt the wind interpretation, since it also allows one to explain the X-ray afterglow. So far, no other quantitative physical models have been worked out for either the thermal X-ray emission or the X-ray afterglow. Soderberg et al. (2006) and Fan et al. (2006b) have suggested that the afterglow X-ray emission is due to extended activity of the source, for which there is no model or explanation. Ghisellini et al. (2007) suggest, to explain the X-ray afterglow, an *Ansatz* consisting of the ad hoc existence of electrons with some prescribed energy distribution, which is different at different times, to account for the observations, without a model for the dynamics of the plasma or for the electron energy distribution.

We note that the radio afterglow of GRB 060218 discussed by Soderberg et al. (2006) is difficult to explain within the context of the current model. Indeed, as pointed out by Soderberg et al. (2006) and by Fan et al. (2006b), it is difficult to explain the radio afterglow and the X-ray afterglow of GRB 060218 as being due to emission from a single shock wave. These authors have thus chosen to construct models that account for the radio emission only, attributing the X-ray afterglow to a continued activity of the source of an unexplained nature, and not accounting for the prompt X-ray emission and for the early optical-UV emission. We adopt a different approach, showing that the prompt (thermal and nonthermal) X-ray emission, the early optical-UV emission, and the late X-ray afterglow can all be explained within the context of the same model. We argue that it is the radio afterglow, rather than all the other components, that remains unexplained and that should be attributed to a different component. Since the radio emission carries only a negligible fraction of the energy, and given the large anisotropy of the explosion, it is not difficult to imagine the existence of such an additional low-energy component.

In § 2 we discuss the observations and our model. In § 3 we compare our analysis with those of other authors. Our results and conclusions are discussed in § 4.

2. OBSERVATIONS AND MODEL

2.1. *Thermal X-Ray Emission: Shock Breakout*

Possibly the most distinguishing feature of GRB 060218 is the strong thermal X-ray emission accompanying the prompt non-thermal emission. The temperature of the thermal X-ray photons

[1] Faculty of Physics, Weizmann Institute of Science, Rehovot 76100, Israel.
[2] Department of Astronomy and Astrophysics and Department of Physics, Pennsylvania State University, University Park, PA 16802.
[3] INAF–Osservatorio Astronomico di Brera, 23807 Merate (LC), Italy.

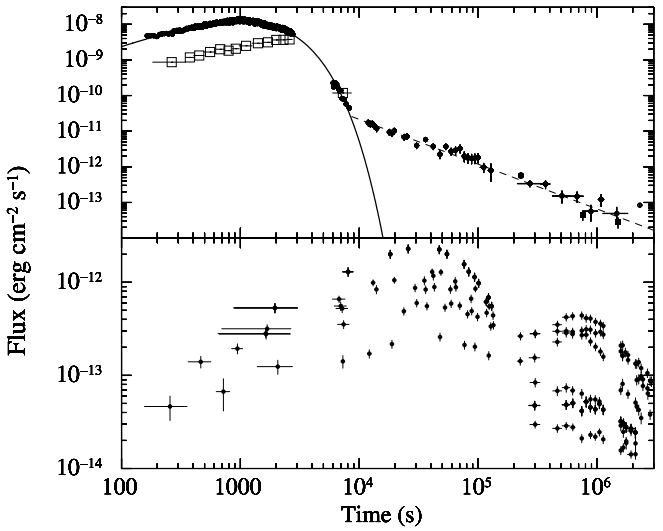

FIG. 1.—*Top*: X-ray light curve (0.3–10 keV). Open circles mark *Swift* XRT data, filled squares indicate *Chandra* data (Soderberg et al. 2006), and the filled circle represents *XMM-Newton* data (De Luca 2006). Open squares denote the blackbody component. A smooth burst with exponential decay fits the prompt part (*solid line*). A power-law decay with index −1.25 well describes the afterglow tail (*dashed line*). Count rate–to–flux conversion factors were derived from time-dependent spectral analysis. The X-ray light curve has a long, slow power-law rise followed by an exponential (or steep power law) decay. At about 10,000 s the light curve breaks to a shallower power-law decay with index -1.2 ± 0.1. *Bottom*: UVOT light curve. Filled circles of various colors represent different UVOT filters (from bottom to top, between 10^4 and 10^5 s): *V* (centered at 544 nm), *B* (439 nm), *U* (345 nm), UVW1 (251 nm), UVM1 (217 nm), and UVW2 (188 nm). Specific fluxes have been multiplied by their FWHM widths (75, 98, 88, 70, 51, and 76 nm, respectively). [*See the electronic edition of the Journal for a color version of this figure*.]

observed up to 3×10^3 s is $T \approx 0.17$ keV (Campana et al. 2006). The integrated flux of the blackbody X-ray component, 6×10^{-6} erg cm^{-2} (see Fig. 1), corresponds (using $d = 145$ Mpc, and after correcting for the flux that falls outside the *Swift* X-Ray Telescope [XRT] band) to a thermal X-ray energy of $E_{\rm th} \approx 2 \times 10^{49}$ erg. This is only an approximate estimate, and the total thermal energy may be somewhat larger, due to the gap in XRT observations between 3×10^3 s and 6×10^3 s. We consider here a model where this radiation is due to a "shock breakout."

Supernova (SN) shock waves become radiation-mediated when propagating through the stellar envelope (see Woosley & Weaver [1986] for a review). The energy density behind the shock is dominated by radiation, and the mechanism that converts kinetic energy to thermal energy at the shock transition is Compton scattering. The optical depth of the shock transition layer is $\tau_s \simeq c/v_s$, where v_s is the shock velocity. This thickness is determined by the requirement that the time it takes a fluid element to flow through the transition layer, $\sim\Delta_s/v_s$, should be comparable to the diffusion time of photons across this layer, $\simeq\tau_s\Delta_s/c$. As the shock propagates outward, the (Thomson) optical depth of the plasma lying ahead of the shock decreases, and when this optical depth becomes comparable to τ_s, Compton scattering can no longer maintain the shock. At this point, radiation escapes ahead of the shock, producing the shock breakout flash (Colgate 1974; Klein & Chevalier 1978; Ensman & Burrows 1992; Matzner & McKee 1999), and the shock becomes collisional (or collisionless; see Waxman & Loeb 2001).

Hereafter we use the term "shock breakout" to denote the event of the transition from radiation to collisional (or collisionless) shock mediation, accompanied by the emission of radiation. If the optical depth of the wind surrounding the progenitor star is small, shock breakout will take place as the shock approaches the stellar surface. It is for this reason customary to identify shock breakout with the emergence of the shock from the stellar surface. However, if the optical depth of the wind is large, $>\tau_s$, breakout would occur once the shock reaches a radius where the wind optical depth drops to τ_s.

As argued in Campana et al. (2006), in order to obtain a breakout flash with an energy of $E_{\rm th} \simeq 10^{49}$ erg and a temperature of $T \approx 0.17$ keV, breakout must occur at a radius of $r \sim 5 \times 10^{12}$ cm, and the shock must be mildly relativistic (which implies that $\tau_s \simeq 1$). Since the progenitor star is presumably smaller than this (e.g., if it is a Wolf-Rayet star), a value of $\tau \simeq 1$ at $r \sim 5 \times 10^{12}$ cm can be obtained by assuming either that the progenitor is surrounded by a dense wind or that an outer shell of the star was ejected to this radius prior to the gamma-ray burst (GRB) explosion. The mass of the shell required to obtain $\tau_s \simeq 1$ is only $\sim 4\pi r^2/\kappa \sim 10^{-6}\ M_\odot$, where $\kappa = 0.2$ g cm^{-2} is the Thomson opacity for ionized He. For the calculation below, we adopt a density profile of $\rho \propto r^{-2}$, as would be expected for the wind model. The results obtained for the breakout radius, shock velocity, and plasma density at this radius are not sensitive, however, to the details of the density profile shape.

We consider, therefore, a shock wave of velocity βc driven into the wind surrounding the progenitor, whose 4-velocity is $u \equiv \gamma\beta$, where $\gamma = (1 - \beta^2)^{-1/2}$ is the Lorentz factor. Let us first derive the energy and temperature of the postshock radiation. The postshock temperature T_d is related to the postshock pressure by $aT_d^4 = 3p$, and the observed temperature is given by $\gamma_d T_d$, where $\gamma_d = (1 - \beta_d^2)^{-1/2}$ and $\beta_d c$ is the postshock plasma velocity ($\beta_d < \beta$). For a strong radiation-dominated shock, $p = fu^2\rho c^2$, where ρ is the preshock density and $f(u)$ is a factor of order unity. As we show below, the shock is required to be mildly relativistic, with u equal to a few, for which we can approximate $f = 0.8$ (for $u \gg 1$, $f = 2/3$) and $(u_d/u)^2 \approx 0.6$ [$(u_d/u)^2 = 1/2$ for $u \gg 1$]. This defines the observed temperature, T, to be

$$T \simeq 1 u^{3/2} (a^{-1}\rho c^2)^{1/4} \tag{1}$$

(for $u \gg 1$, the numerical coefficient is $1/2^{1/4}$ instead of 1). The energy carried by the radiation can be estimated by noting that the energy density of the radiation is given, in the observer frame, by $-p + \gamma_d^2(aT_d^4 + p) = (4u_d^2 + 3)p$, and that the thickness of the shocked plasma shell can be approximated as $d = (\beta - \beta_d)r$, where r is the shock radius. This yields

$$\frac{E_{\rm th}}{4\pi r^3 \rho c^2} = (\beta - \beta_d)(4u_d^2 + 3)\frac{p}{\rho c^2} \simeq 0.5u^2 \tag{2}$$

(for $u \gg 1$, the numerical coefficient is 2/3 instead of 0.5).

For a wind density profile, the optical depth of the wind at radius r is simply $\tau(r) = \kappa\rho(r)r$. Expressing the density in terms of $\tau(r)$ and using equations (1) and (2), we find that the shock velocity at breakout is

$$u^2 = \left(\frac{aT^4}{\sqrt{2\pi}c^3}\right)^{1/7}\left(\frac{\kappa}{\tau}\right)^{3/14} E_{\rm th}^{1/14} = 2.5\left(\frac{T}{0.17\ {\rm keV}}\right)^{4/7} E_{\rm th,\,49}^{1/14}, \tag{3}$$

and that breakout occurs at a radius

$$R_{\rm ph} = \left[\frac{E_{\rm th}^3}{(2\pi)^3 a T^4 c^4}\right]^{1/7} \left(\frac{\kappa}{\tau}\right)^{2/7} = 7.8\times10^{12}\left(\frac{T}{0.17\ {\rm keV}}\right)^{-4/7} E_{\rm th,\,49}^{3/7}\ {\rm cm}, \quad (4)$$

where $E_{\rm th} = 10^{49} E_{\rm th,\,49}$ erg and we have used $\kappa = 0.2$ g cm^{-2} and $\tau = 1$ in the numerical evaluations. Note that the results depend only weakly on the exact values of κ and τ.

Equations (3) and (4) imply that the breakout of the shock takes place at a radius of $\simeq 7.8\times10^{12}$ cm and that the shock is mildly relativistic at breakout, $u^2 = 2.5$; i.e., $\beta = 0.85$. These results are in agreement with the order-of-magnitude estimates given in Campana et al. (2006). Since the shock is found to be mildly relativistic, using $\tau = 1$ at shock breakout is justified. In order to produce the shock that is driven into the wind, the explosion is thus required to produce a mildly relativistic shell, $\beta = 0.8$, with an energy of a few times 10^{49} erg. This is remarkably similar to the case of GRB 980425/SN 1998bw, for which the ejection of a shell of energy $10^{49.7}$ erg and velocity $\beta = 0.8$ was inferred from X-ray (Waxman 2004b) and radio (Kulkarni et al. 1998; Waxman & Loeb 1999; Chevalier & Li 1999; Waxman 2004a) observations.

The wind density at the breakout radius, $\rho = 1/\kappa r = 10^{-12}$ g cm^{-3}, is also in agreement with our results in Campana et al. (2006). It is straightforward to verify that the energy density is dominated by radiation: $aT^4/nT \sim 10^9$. For a wind velocity of $\sim 10^3$ km s^{-1}, it corresponds to a mass-loss rate of a few times $10^{-4}\,M_\odot$ yr^{-1}. The relevant mass loss here is that occurring within a day or less after the explosion. The data currently available on wind mass losses that suggest $\dot{M} \lesssim$ a few $\times\, 10^{-4}\,M_\odot$ yr^{-1} refer to much longer timescales, for stars well before any explosion (Meynet & Maeder 2007). Physically, it is however quite plausible that the mass loss increases considerably as the evolution of the core rapidly approaches the final collapse, accompanied by a rapid increase in the luminosity and the envelope expansion rate.

Note that if both the shell and the wind were spherically symmetric, the characteristic timescale would be $R_{\rm ph}/c = 260$ s (for the inferred postshock velocity, $\gamma_d\beta_d = 1.2$, the effects of relativistic beaming are not significant), while the observed timescale of the thermal X-ray emission is $\sim 10^3$ s (Campana et al. 2006). However, an anisotropic shell ejection is a natural expectation in a core-collapse GRB, since strong rotation is a requisite to make the jet (e.g., MacFadyen & Woosley 1999). Even "normal" core-collapse SN simulations show strong rotation-related anisotropy in the expanding gas (e.g., Burrows et al. 2007). Thus, the semirelativistic outer shell ejected is likely to be anisotropic, either due to an anisotropic explosion, or due to being driven by a jet. This, as well as an anisotropic wind profile caused by rotation (Meynet & Maeder 2007), should lead to significant departures from sphericity in the shock propagation. Anisotropy is in fact a prediction of this model, which is supported by the detection of linear polarization (Gorosabel et al. 2006). In an anisotropic shock, however, the timescale is no longer the naive spherical r/c value, but is rather given by the sideways pattern expansion timescale, which depends on the angular velocity profile of the anisotropic shell (e.g., at larger angles, the shock emerges later, due to a decreasing velocity profile or an increasing wind density away from the symmetry axis).

2.2. *X-Ray Afterglow: Wind-Shell Interaction*

If the wind shock breakout interpretation is adopted, the subsequent interaction of the ejected relativistic shell with the wind is expected to produce an X-ray afterglow (Waxman 2004b). The electrons accelerated to high energy in the collisionless shock driven into the wind emit X-ray synchrotron radiation, and may also inverse Compton scatter optical-UV supernova photons to the X-ray band.

As the shock wave driven into the wind expands, it heats an increasing amount of mass to a high temperature, and the initial energy of the ejected shell is transferred to the shocked wind. The shell begins to decelerate beyond a radius at which the shocked wind energy becomes comparable to the initial shell energy. This occurs at a time (Waxman 2004b)

$$t_{\rm dec} = 0.06\frac{E_{k,\,49}}{\beta^3(\dot{m}/10)}\ {\rm days}. \quad (5)$$

Here $E_k = 10^{49} E_{k,\,49}$ erg is the kinetic energy of the shell and

$$\dot{m} \equiv \frac{\dot{M}/v_w}{10^{-5}(M_\odot\ {\rm yr}^{-1})/10^3({\rm km\ s}^{-1})}. \quad (6)$$

For the wind density and shell velocity inferred in § 2.1, $\beta = 0.85$ and $\dot{m} \gtrsim 10$, $t_{\rm dec} \lesssim 10^4$ s. At $t > t_{\rm dec}$ the energy is carried by the shocked wind plasma and is continuously transferred to a larger mass of newly shocked parts of the wind. Thus, the rate at which energy is transferred to accelerated electrons is $\approx \epsilon_e E_k/t$, where ϵ_e is the fraction of the postshock thermal energy carried by electrons. If the electrons cool on a timescale shorter than the expansion time, $\sim t$, this would lead to a bolometric luminosity of $L_B \approx 10^{43}\epsilon_{e,-1}E_{k,49}(t/1\ {\rm day})^{-1}$ erg cm^{-2} s^{-1}. The fraction of this luminosity emitted as X-rays depends on the electron energy distribution. For electrons accelerated to a power-law distribution in energy, $d\log n_e/d\log\gamma_e \approx -2$,

$$\nu L_\nu \approx \frac{L_B}{2\log(\gamma_{\rm max}/\gamma_{\rm min})} \approx 10^{42}\epsilon_{e,\,-1}E_{k,\,49}\left(\frac{t}{1\ {\rm day}}\right)^{-1}\ {\rm erg\ cm^{-2}\ s^{-1}},$$

where $\gamma_{\rm max}$ and $\gamma_{\rm min}$ are the maximum and minimum electron Lorentz factors, respectively. The more detailed analysis given in Waxman (2004b) of the synchrotron emission of shock accelerated electrons gives (eqs. [6] and [7] of Waxman 2004b)

$$\nu L_{\nu,{\rm synch}} \approx 3\times10^{41}\epsilon_{e,\,-1}E_{k,\,49}t_d^{-1}\ {\rm erg\ s^{-1}} \quad (7)$$

for

$$\nu > \nu_c \approx 3\times10^{10}\epsilon_{B,\,-1}^{-3/2}(\dot{m}/10)^{-3/2}t_d\ {\rm Hz}. \quad (8)$$

Here $t = 1t_d$ days, $\epsilon_e = 10^{-1}\epsilon_{e,\,-1}$ and $\epsilon_B = 10^{-1}\epsilon_{B,\,-1}$ are the fractions of the postshock thermal energy carried by electrons and the magnetic field, respectively, and ν_c is the cooling frequency, the frequency of synchrotron photons emitted by electrons for which the synchrotron cooling time equals t (higher energy electrons cool faster and emit higher energy photons). Equation (7) implies an X-ray luminosity in the *Swift* XRT band, 0.3–10 keV, of

$$L_{\rm X,synch} \approx 10^{42}\epsilon_{e,\,-1}E_{k,\,49}t_d^{-1}\ {\rm erg\ s^{-1}}. \quad (9)$$

Let us consider next the inverse Compton scattering of SN optical-UV photons by the shock-heated electrons. The inverse Compton (IC) luminosity emitted by electrons with Lorentz factor γ_e is given by $L_{\rm IC} \approx \gamma_e^2 \tau(\gamma_e) L_{\rm SN}$, where $\tau(\gamma_e)$ is the Thomson optical depth of these electrons and $L_{\rm SN}$ is the SN luminosity. The lowest energy IC photons are produced by the lowest energy (thermal) electrons, $(h\nu)_{{\rm IC},T} \approx (4\gamma_T^2/3)2$ eV, where γ_T is the Lorentz factor of the lowest energy electrons. The quantity γ_T is determined from the postshock thermal energy density, $[2/(\Gamma^2 - 1)]\rho v_s^2 \approx \rho v_s^2$, where v_s is the shock velocity and $\rho = \dot{M}/4\pi r^2 v_w$ ($\Gamma \approx 5/3$ is the adiabatic index), through $\Lambda n_e \gamma_T m_e c^2 = \epsilon_e \rho v_s^2$. Here Λ is a dimensionless constant, the value of which depends on the exact form of the electron energy distribution. For a power-law distribution, $d\log n_e/d\log\gamma_e \approx -2$, $\Lambda \approx \log(\gamma_{\rm max}/\gamma_{\rm min})$. The shock velocity can be inferred from the shock radius, which is given by (eq. [2] of Waxman 2004b)

$$R_s = 0.73\left(\frac{E_k}{\dot{M}/4\pi v_w}t^2\right)^{1/3} = 1.8\times10^{15}\left(\frac{E_{k,49}}{\dot{m}/10}\right)^{1/3} t_d^{2/3}\ {\rm cm}. \quad (10)$$

Using $v_s = (2/3)R_s/t$, we find

$$\gamma_T \approx 80\epsilon_{e,-1}\Lambda^{-1}\left(\frac{E_{k,49}}{\dot{m}/10}\right)^{2/3} t_d^{-2/3}, \quad (11)$$

$$(h\nu)_{{\rm IC},T} \approx 15\epsilon_{e,-1}^2\Lambda^{-2}\left(\frac{E_{k,49}}{\dot{m}/10}\right)^{4/3} t_d^{-4/3}\ {\rm keV}. \quad (12)$$

Thus, on a timescale of a day, IC scattering by the lowest energy (thermal) electrons is expected to contribute to the X-ray flux. It is important to note here that the electrons producing the X-ray synchrotron flux, shown in equation (9), are of much higher energies, $\gamma_e \gg \gamma_T$, and lie at the high-energy part of the accelerated electron energy distribution.

The Thomson optical depth of the thermal electrons is approximately given by $\kappa M(r)/4\pi r^2 = \kappa\rho r$, where $M(r)$ is the wind mass accumulated up to r. If we assume that the thermal electrons do not lose all their energy by IC scattering on a timescale shorter than the expansion time t, the IC luminosity produced by the thermal electrons is

$$L_{{\rm IC},T} \approx \kappa\rho r\gamma_T^2 L_{\rm SN} \approx 9\times10^{42}\frac{\epsilon_{e,-1}^2}{\Lambda^2}E_{k,49}\frac{L_{\rm SN}}{10^{42.5}\ {\rm erg\ s^{-1}}}t_d^{-2/3}\ {\rm erg\ s^{-1}}. \quad (13)$$

The IC luminosity given by equation (13) may exceed, depending on the values of Λ and ϵ_e, the luminosity given by equation (9). However, $L_{{\rm IC},T} > L_{\rm X,\,synch}$ is not, of course, a valid result, since the quantity $L_{\rm X,\,synch}$ given in equation (9) is the luminosity obtained by assuming that the electrons lose to radiation all the energy that they gained from the shock. The IC luminosity is thus limited by $L_{\rm X,\,synch}$, and $L_{{\rm IC},T} > L_{\rm X,\,synch}$ simply implies that the thermal electrons lose all their energy to IC scattering on a short timescale.

Let us compare the predicted X-ray afterglow with the observed one. The observed X-ray afterglow, following the prompt emission, which ends at $\sim10^4$ s, is well approximated by (see Fig. 1) $f_{\rm X} = 10^{-12}t_d^{-1.2\pm0.1}$ erg cm^{-2} s^{-1}, which corresponds to $L_{\rm X} = 2\times10^{42}t_d^{-1.2\pm0.1}$ erg s^{-1}. This is in excellent agreement with the predictions of equations (9) and (13) for $E_k =$ a few $\times$ 10^{49} erg. The fact that the energy of the shock driven into the wind that is inferred from the X-ray afterglow, E_k, is comparable to that of the thermal X-rays, $E_{\rm th}$, supports our model, in which both are due to the same shock driven into the wind.

At early times, $t < 1$ day, the emission is expected to be dominated by the synchrotron component, and for the power-law energy distribution of electrons, $d\log n_e/d\log\gamma_e \approx -2$, the X-ray spectrum is expected to follow $\nu L_\nu \propto \nu^0$. On a timescale of a few days, the emission is expected to be dominated by IC scattering of thermal SN photons by thermal shock electrons. At this stage, the X-ray spectrum may become steeper, reflecting the energy distribution of the lowest energy electrons heated by the shock. These results are consistent with the $\nu L_\nu \propto \nu^0$ X-ray spectrum measured at $t \sim 1$ day, and with the indication, based on an *XMM-Newton* observation, that at a later time, $t \sim 3$ days, the spectrum is steeper, $\nu L_\nu \propto \nu^{-1.3\pm0.6}$ (De Luca 2006).

The following point should be made here. As the shock speed $\dot{R}_s$ decreases with time, shells ejected with velocities lower than that of the fast ($\beta \simeq 0.8$) shell may "catch up" with the shock ($R_s/ct = 0.6t_d^{-1/3}$ for $E_{k,49} = 1$ and $\dot{m} = 10$). This may lead to an increase with time of the shock kinetic energy E_k and thus to a modification of the X-ray light curve. The fact that the X-ray luminosity decreases roughly as $1/t$ for up to $\sim$10 days implies that the energy in shells ejected with $\beta \gtrsim 0.3$ is not much larger than that of the fast shell; i.e., not much larger than 10^{49} erg.

2.3. *Early Optical-UV Emission: Envelope Cooling*

As the SN shock propagates through the stellar envelope, it heats it to $\sim$1 keV. As the envelope expands, the photosphere propagates into the envelope, and we see deeper shells with lower temperatures. We derive here a simple analytic model for the photospheric radius and temperature, on the basis of which we can derive approximately the flux and temperature of the escaping radiation. We assume that the density of the stellar envelope near the stellar surface is given by

$$\rho_0(r) = \rho_{1/2}\delta^n, \quad (14)$$

where $\delta \equiv (1 - r/R_*)$ (R_* is the stellar radius), and that the plasma ahead of the photosphere is highly ionized He, so that $\kappa = 0.2$ cm^2 g^{-1}. The velocity of the shock as it propagates through the envelope is approximately given by (Matzner & McKee 1999; Tan et al. 2001)

$$v_s = 0.8\left(\frac{E_{\rm ej}}{M_{\rm ej}}\right)^{1/2}\left(\frac{M_{\rm ej}}{\rho r^3}\right)^{0.2} \underset{r\to R_*}{\longrightarrow} 0.8\left(\frac{E_{\rm ej}}{M_{\rm ej}}\right)^{1/2}\left(\frac{M_{\rm ej}}{\rho_{1/2}R_*^3}\right)^{0.2}\delta^{-0.2n}, \quad (15)$$

where $M_{\rm ej}$ is the mass of the ejected envelope and $E_{\rm ej}$ is the energy deposited in the envelope. Since the shock is radiation-dominated, the energy density behind the shock is given by $u_{{\rm rad},0}/3 = (6/7)\rho_0 v_s^2$:

$$aT_0^4(\delta) = u_{{\rm rad},0}(\delta) = \frac{18}{7}\rho_0(\delta)v_s(\delta)^2. \quad (16)$$

After the shock breaks through the envelope, the envelope begins to expand and cool. It is useful to label the shells with Lagrangian coordinates, defining $\delta_m(\delta)M_{\rm ej}$ as the (time-independent) mass that lies ahead of a shell originally located at $r = (1 - \delta)R_*$. Matzner & McKee (1999) show that the final velocity (after acceleration due to the adiabatic expansion) of each shocked shell,

v_f, is related to the shock velocity approximately by $v_f(\delta_m) = 2v_s[\delta(\delta_m)]$. After significant expansion, $v_f t \gg R_*$, the radius of each shell is given by $r(\delta_m, t) = v_f(\delta_m)t$. Given $r(\delta_m, t)$ it is straightforward to derive the time-dependent shell density. The shell's (time-dependent) temperature is then determined by $T/T_0 = (\rho/\rho_0)^{4/3}$, which holds for adiabatic expansion. After some tedious algebra we find that, for $v_f t \gg R_*$, the photosphere is located at

$$\delta_{m,\,\mathrm{ph}}(t) = 3.8 \times 10^{-3} f_\rho^{-0.07} \frac{E_{\mathrm{ej},\,51}^{0.8}}{(M_{\mathrm{ej}}/M_\odot)^{1.6}} t_d^{1.6}. \quad (17)$$

Here $E_{\mathrm{ej}} = 10^{51} E_{\mathrm{ej},\,51}$ erg and $f_\rho \equiv \rho_{1/2}/\bar{\rho}_0$ is the ratio between $\rho_{1/2}$ and the average envelope density $\bar{\rho}_0$. Although f_ρ depends on the structure of the progenitor star far from the surface, where equation (14) no longer holds, the results are very insensitive to its value. Using equation (15), we find that the radius of the photosphere is

$$r_{\mathrm{ph}}(t) = 3.2 \times 10^{14} f_\rho^{-0.04} \frac{E_{\mathrm{ej},\,51}^{0.4}}{(M_{\mathrm{ej}}/M_\odot)^{0.3}} t_d^{0.8}\ \mathrm{cm}, \quad (18)$$

and using equation (16), we find that the temperature of the photosphere is

$$T_{\mathrm{ph}}(t) = 2.2 f_\rho^{-0.02} \frac{E_{\mathrm{ej},\,51}^{0.02}}{(M_{\mathrm{ej}}/M_\odot)^{0.03}} R_{*,\,12}^{1/4} t_d^{-0.5}\ \mathrm{eV}. \quad (19)$$

Here $R_* = 10^{12} R_{*,\,12}$ cm.

Campana et al. (2006) find $R \approx 3 \times 10^{14}$ cm and $T \approx 3$ eV at $t = 10^5$ s. This is clearly consistent with the cooling envelope interpretation. We note that at $t = 10^5$ s the emission originates from a shell of mass $\simeq 10^{-3}\, M_\odot$, in excellent agreement with our rough estimate in Campana et al. (2006). At the time $t \ll 10^5$ s, optical photons are in the Rayleigh-Jeans tail, and the flux is approximately given by $f_\nu \approx 2\pi(\nu/c)^2 T_{\mathrm{ph}}(r_{\mathrm{ph}}/D)^2$, where D is the distance to GRB 060218. Using equations (18) and (19), we find

$$\nu f_\nu \approx 1.3 \times 10^{-13} f_\rho^{-0.1} \frac{E_{\mathrm{ej},\,51}^{0.8}}{(M_{\mathrm{ej}}/M_\odot)^{0.6}} R_{*,\,12}^{1/4} \times \left(\frac{\nu}{5 \times 10^{14}\mathrm{Hz}}\right)^3 t_4^{1.1}\ \mathrm{erg\ cm^{-2}\ s^{-1}}, \quad (20)$$

where $t = 10^4 t_4$ s. This is consistent with the optical flux observed at early times; see Figure 1 (note that our derivation holds only for $r_{\mathrm{ph}} \gg R_*$; i.e., for $t > 10^3$ s).

A more detailed study of the optical-UV early light could provide interesting constraints on the size and density distribution near the surface of the progenitor star. Such a detailed analysis would require taking into account effects neglected here (e.g., photon diffusion, which may be important on >1 day timescales; anisotropy) and is beyond the scope of the current manuscript.

Note that we have neglected the effects of photon diffusion in the above derivation. We do not expect diffusion to play an important role, due to the following argument. The size of a region around $r(\delta_m, t)$ over which diffusion has a significant effect is $\Delta(\delta_m, t) = [ct/3\kappa\rho(\delta_m, t)]^{1/2}$. Thus, the value of δ_m up to which diffusion affects the radiation field significantly, δ_D, is determined by $\Delta(\delta_m = \delta_D, t)/r(\delta_m = \delta_D, t) = 1$, which gives

$$\frac{r(\delta_m = \delta_D, t)}{r_{\mathrm{ph}}} = 1.2 f_\rho^{-0.005} \frac{E_{\mathrm{ej},\,51}^{0.05}}{(M_{\mathrm{ej}}/M_\odot)^{0.03}} t_d^{-0.03}. \quad (21)$$

This implies that photon diffusion is not expected to significantly modify the predicted light curve. (Applying, e.g., the approximate self-similar diffusion wave solutions of Chevalier [1992] to our density and velocity profiles yields a luminosity that differs by <25% from that derived neglecting diffusion.)

2.4. *Radio Emission*

For the massive wind discussed in our model, the synchrotron self-absorption optical depth is very large at radio frequencies. The characteristic frequency of synchrotron photons emitted by the lowest energy, $\gamma_e \sim \gamma_T$, electrons is $\nu_m \approx \gamma_T^2 eB/2\pi m_e c$, where the magnetic field is given by $B^2/8\pi = \epsilon_B \rho v_s^2$. Using equations (10) and (11), we have

$$\nu_m \approx 5 \times 10^{11} \Lambda^{-2} \epsilon_{B,\,-1}^{1/2} \epsilon_{e,\,-1}^2 E_{k,\,49}^{4/3} (\dot{m}/10)^{-5/6} t_d^{-7/3}\ \mathrm{Hz}. \quad (22)$$

On a timescale of a few days, we therefore expect the radio frequency, $\nu \sim 10$ GHz, to be in the range $\nu_m \lesssim \nu < \nu_c$ (see eq. [8]); i.e., we expect the Lorentz factor of electrons dominating the emission and absorption of radio waves to be in the range $\gamma_T \lesssim \gamma_\nu < \gamma_c$ (where γ_c is the Lorentz factor of electrons with a cooling time comparable to the expansion time). In this case, the synchrotron self-absorption optical depth is given by $\tau_\nu = [e^3 B/2\gamma_\nu(m_e c\nu)^2] n_e(\gamma_\nu)\Delta$, where $n_e(\gamma_\nu)$ is the number density of electrons with Lorentz factor γ_ν and Δ is the thickness of the shocked wind shell. For a power-law distribution, $dn_e/d\gamma_e \propto \gamma_e^{-2}$, we have $n_e(\gamma_\nu) \approx n_e \gamma_T/\gamma_\nu$, and, using $n_e\Delta = \rho r/2m_p$ for the electron column density, we have

$$\tau_\nu \approx 10^7 \frac{\epsilon_{B,\,-1}\epsilon_{e,\,-1}}{\Lambda} E_{k,\,49}^{1/3} (\dot{m}/10)^{5/3} \left(\frac{\nu}{10\ \mathrm{GHz}}\right)^{-3} t_d^{-10/3}. \quad (23)$$

This large optical depth leads to a strong suppression of the radio synchrotron flux, compared to the X-ray synchrotron flux given in equation (7):

$$\frac{(\nu L_\nu)_{\mathrm{radio}}}{(\nu L_\nu)_{\mathrm{X}}} \approx 10^{-4} \frac{\Lambda}{\epsilon_{B,\,-1}^{1/4}\epsilon_{e,\,-1}} E_{k,\,49}^{-1/3} (\dot{m}/10)^{-11/12} \times \left(\frac{\nu}{10\ \mathrm{GHz}}\right)^{7/2} (t_d/10)^{17/6}. \quad (24)$$

The flux ratio measured at a few to 20 days is $(\nu L_\nu)_{\mathrm{radio}}/(\nu L_\nu)_{\mathrm{X}} \approx 10^{-2.5}$ (Soderberg et al. 2006). Thus, as noted in the Introduction (§ 1), the observed radio flux is higher than that predicted by this model and should be explained as a different component (see also § 3.3).

3. COMPARISON WITH OTHER AUTHORS

3.1. *Ghisellini et al. (2007)*

Ghisellini et al. (2007) argue that the shock breakout interpretation is not valid, since the optical-UV emission at a few times 10^3 s is higher than the extrapolation to low frequencies of the Planck spectrum that fits the thermal X-ray emission at the same time. As we have pointed out in Campana et al. (2006), and as is explained in detail in § 2, the thermal X-ray emission and the early optical-UV emission originate from different regions. The

thermal X-rays originate from a (compressed) wind shell of mass $\sim 10^{-6}\, M_\odot$, while the optical-UV emission originates from the outer shells of the (expanding) star. At $\sim 10^4$ s the optical-UV radiation is emitted from a shell at a "depth" of $\sim 10^{-4}\, M_\odot$ from the stellar edge. The optical-UV and the thermal X-rays need not correspond to the same Planck spectrum. As we have explained in Campana et al. (2006), and in more detail in § 2, if the explosion had been isotropic, the thermal X-ray emission should have disappeared altogether on a timescale of a few hundred seconds, the time at which Ghisellini et al. (2007) compare the X-ray and UV emission. The fact that the thermal X-ray emission is observed over a few thousand seconds can be accounted for by assuming an anisotropic explosion. This assumption, made explicitly both in Campana et al. (2006) and here, is ignored by Ghisellini et al. (2007), whose criticism is framed in the context of a spherical model, which we never assumed.

Concerning their own model, in their preferred explanation for the properties of this burst, Ghisellini et al. (2007), unlike in our model, do not include any dynamics in their scenario, and they adopt different ad hoc parameters (e.g., for the electron distribution) at different times to account for the observations.

3.2. *Li* (*2007*)

Li (2007) argues that in order to explain the "temperature and the total energy of the blackbody component observed in GRB 060218 by the shock breakout, the progenitor WR star has to have an unrealistically large core radius . . . larger than $100\, R_\odot$." The results of Li (2007) are in fact consistent with our analysis. The "core radius," R_c, adopted by this author refers not to the hydrostatic core radius of the star, but rather to the radius at which the optical depth equals 20. In non-LTE modeling of the winds of WR stars, R_c is located within the wind, typically near the sonic point. In fact, in some cases the wind velocity is already supersonic at R_c (e.g., Hamann & Koesterke 1998). Thus, R_c is much larger than the hydrostatic core radius $R_{\rm hc}$ obtained in evolutionary calculations (e.g., Schaerer & Maeder 1992). As shown by Nugis & Lamers (2002), $R_c/R_{\rm hc}$ varies with the spectral type of WR stars, increasing from about 2 for early types to about 20 for late types (see Table 5 of Nugis & Lamers 2002).

Since Li (2007) considers in his calculations models in which the ratio between the wind photospheric radius $R_{\rm ph}$ and R_c is $1 < R_{\rm ph}/R_c < 3$ (using his notation, for $b = 5$, the choice of $\epsilon = 10^{-5}$–10^{-2} corresponds to $1 < R_{\rm ph}/R_c < 3$; see his Fig. 3), his statement that $R_c \sim 100\, R_\odot$ is required implies that a wind with a photospheric radius of 7×10^{12}–2×10^{13} cm is needed to account for the thermal X-ray emission of GRB 060218 as shock breakout. This is consistent with our equation (4).

It is important to emphasize that the relevant radius is not R_c, but rather the wind photospheric radius, $R_{\rm ph}$, where $\tau = 1$. It is the photospheric radius that needs to be large in order to allow a sufficiently large shock breakout energy. The quantity $R_{\rm ph}$ is larger than R_c by a factor of 2–10, depending on the model adopted for the wind velocity profile. Nugis & Lamers (2002) present late-type models with $R_c/R_\odot > 30$, and a large fraction of the stars analyzed in Hamann & Koesterke (1998) have $R_c/R_\odot > 25$ (see their Table 2). Values of $R_{\rm ph}$ larger than $100\, R_\odot$ can therefore be obtained for stars with large mass-loss rates.

It should be emphasized that, even if the wind photospheric radius required for GRB 060218 had turned out to be larger by a factor of a few than the largest $R_{\rm ph}$ of known WR stars, this would not have been a strong argument against the wind interpretation of GRB 060218, since GRB progenitors may well be more extreme than normal WR stars. Clearly, not all WR stars end their lives as GRBs. Moreover, it should be remembered that practically nothing is known about the mass loss on a day timescale prior to the explosion, which determines the wind density at the relevant radii.

3.3. *Fan et al.* (*2006b*)

Fan et al. (2006b) raised different criticisms in different versions of their paper. In the first version, Fan et al. (2006a), they argued that the presence of a massive wind would result in strong optical emission at early times, which is inconsistent with observations. While this claim was retracted in subsequent versions of their manuscript, it may be worthwhile to clarify this issue here. The synchrotron emission given in equation (7) holds for frequencies above the cooling frequency, $\nu > \nu_c$. Since the cooling frequency is low for a massive wind (see eq. [8]), we expect in this model a similar X-ray and optical-UV luminosity, $\nu f_\nu \approx 3 \times 10^{-13} (t/1\ {\rm day})^{-1}\ {\rm erg\ cm^{-2}\ s^{-1}}$ [corresponding to a flux of $F_{\rm UV} \approx 1 \times 10^{-13} (t/1\ {\rm day})^{-1}\ {\rm erg\ cm^{-2}\ s^{-1}}$ in the 0.2 μm band of the *Swift* UV/Optical Telescope (UVOT)]. This predicted flux exceeds the observed flux at $t < 10^4$ s; hence the statement of Fan et al. (2006b). However, as pointed out in § 2.2, equation (7) holds only for times $t > t_{\rm dec} \sim 10^4$ s (and the luminosity is lower at earlier times). Moreover, at $t < 10^4$ s, the large X-ray luminosity, $L_{\rm X} \sim 10^{46}\ {\rm erg\ s^{-1}}$, would suppress the synchrotron emission of the shock-accelerated electrons. As explained in § 2.2, the cooling time of shock-accelerated electrons due to synchrotron emission is short compared to the shock expansion time. At early times, $t < 10^4$ s, the ratio of the magnetic energy density, $\epsilon_B E/r^3$, to the X-ray energy density, $L_{\rm X}/4\pi r^2 c$, is

$$4\pi\epsilon_B E c/L_{\rm X} r \sim 10^{-3.5} \epsilon_{B,-1} E_{k,49} (r/10^{15}\ {\rm cm}),$$

which implies that the IC cooling time is much shorter than the synchrotron cooling time, suppressing the synchrotron emission in the optical band.

Second, Fan et al. (2006b) argue (see also Soderberg et al. 2006) that radio observations rule out the existence of a massive wind. As mentioned in the Introduction (§ 1), the radio and the X-ray afterglow are indeed difficult to explain in the framework of a single shock. However, the radio observations alone cannot be used to rule out the existence of a massive wind, since radio observations do not allow one to determine the explosion parameters. This is illustrated by the fact that estimates for the kinetic energy based on modeling the radio data alone range from $\sim 10^{48}$ to $\sim 10^{50}$ erg, and that the ambient medium density estimates range from $\sim 10^0$ to $\sim 10^2\ {\rm cm^{-3}}$ (Fan et al. 2006b; Soderberg et al. 2006).

Finally, Fan et al. (2006b) argue that in the presence of a massive wind, the radio flux would be higher than that observed. As explained in § 2.4, our problem is quite the opposite: our model flux would be too low to account for the observed radio emission. Soderberg et al. (2006) and Fan et al. (2006b) have chosen to construct models of GRB 060218 that concentrate on accounting for the radio emission, while attributing the X-ray afterglow to a continued activity of the source of an unexplained nature, and deemphasizing the importance of the prompt X-ray emission and the early optical-UV emission. However, the radio emission represents a negligible fraction of the total energy. Here and in Campana et al. (2006), we have adopted a different approach, which is that the prompt (thermal and nonthermal) X-ray emission, the early optical-UV emission, and the late X-ray afterglow can all be explained within the context of the same model, which is based on the energetics of the early phases of the

explosion. We argue that it is the radio afterglow, rather than all the other components, that plays a lesser role and that may be attributed to a different component. Given the very low energy of the radio emission and the large anisotropy expected in the explosion, such an additional low-energy radio component is imaginable, whose role is unlikely to be important in determining the characteristics of the early high-energy emission.

4. DISCUSSION

We have discussed a comprehensive model of the early X-ray and optical-UV behavior of the GRB 060218/SN 2006aj system that provides the quantitative justification for the interpretation outlined in Campana et al. (2006), as well as a number of additional points. The most exciting features of this event were that it showed a strong thermal X-ray component, as well as a strong optical-UV component in its early phases, at $t \lesssim 1$ day, that transitioned later to a more conventional X-ray and optical afterglow, and a radio afterglow. We have shown that the early X-ray/optical/UV behavior can be understood in terms of a mildly relativistic radiation-mediated shock that breaks out of a (Thomson) optically thick wind produced by the progenitor star, leading to the observed thermal X-rays (see § 2.1). The early optical-UV behavior arises as the shocked stellar envelope expands to larger radii (§ 2.3), and the X-ray afterglow arises from synchrotron and inverse Compton emission of electrons accelerated by the propagation of the shock further into the wind (§ 2.2). A detailed analysis of the optical-UV emission may therefore provide stringent constraints on the progenitor star.

The thermal X-ray emission requires a mildly relativistic shock, $\beta \approx 0.8$, carrying $\gtrsim 10^{49}$ erg, driven into a massive wind characterized by a mass-loss rate of a few times $10^{-4}\, M_{\odot}\ \mathrm{yr}^{-1}$ for a wind velocity of 10^3 km s^{-1}. The later X-ray afterglow is consistent with emission due to the propagation of this shock into the wind beyond the breakout radius, where the shock becomes collisionless. This situation is very similar to that of GRB 980425/SN 1998bw, for which the X-ray and radio afterglow are interpreted as emission from a shock driven into a (much less massive) wind by the ejection of a shell of energy $10^{49.7}$ erg and velocity $\beta = 0.8$ (Waxman 2004b and references therein).

The early optical-UV emission is consistent with the expansion of the outer part, $\delta M \sim 10^{-3}\, M_{\odot}$, of the stellar envelope, which was heated to a high temperature by the radiation-dominated shock as it accelerated in its propagation toward the stellar edge. It is important to note, however, that the acceleration of the shock near the stellar surface is not sufficient to account for the large energy, $\gtrsim 10^{49}$ erg, deposited in the mildly relativistic, $\beta \approx 0.8$, component, which is required to have a mass of $\sim 10^{-5}\, M_{\odot}$. For the parameters inferred from the SN 2006aj light curve, $E_{\rm ej} \simeq 2 \times 10^{51}$ erg and $M_{\rm ej} \simeq 2\, M_{\odot}$ (Mazzali et al. 2006), the energy predicted to be carried by $\beta \geq 0.8$ is less than 10^{45} erg (see Fig. 6 of Tan et al. 2001). This suggests that the mildly relativistic component is driven not (only) by the spherical SN shock propagating through the envelope, but possibly by a more relativistic component of the explosion, e.g., a relativistic jet propagating through the star.

An important factor in our interpretation of the early X-ray emission is the anisotropy of this shock, which leads to a characteristic timescale of the thermal X-ray emission controlled by the sideways pattern expansion speed, rather than by a simple radial line-of-sight velocity. A significant anisotropy of the mildly relativistic shock component is expected for various reasons, e.g., as a result of being driven by a jet, or due to propagation through an anisotropic envelope and into an anisotropic wind caused by fast progenitor rotation. The simplest explanation for the prompt gamma-ray behavior may be that it is due to a relativistic jet, which could contribute to the anisotropy of the mildly relativistic shock propagating through the stellar envelope and the mildly relativistic ejected shell. In this case, the contribution of the relativistic jet to the late ($t \gtrsim 1$ day) X-ray and optical afterglow is not the dominant effect (cf. Liang et al. 2006). However, a possible explanation of the prompt nonthermal emission, both in GRB 980425 and GRB 060218, may be that it is due to repeated IC scattering at breakout, as suggested in Wang et al. (2007; cf. Dai et al. 2006). In this case there may be no highly relativistic jet; it may either be mildly relativistic to begin with, or it may have been relativistic but it was choked, with only its mildly relativistic bow shock emerging from the star.

If our interpretation is correct, the importance of the early thermal X-ray component is that it represents the first detection ever of the breakout of a supernova shock from the effective photosphere of the progenitor star. Since this is a GRB-related supernova, a strong stellar wind can be expected, which results in the breakout photospheric radius being in the wind, rather than in the outer atmosphere of the star. This provides a potentially valuable tool for investigating the physical conditions, mass loss, and composition of the long GRB progenitors in the last few days and hours of their evolution prior to their core collapse.

We are grateful to our *Swift* colleagues for stimulating collaborations, and to NASA NAG5-13286 (P. M.), ISF and Minerva (E. W.), and ASI I/R/039/04 (S. C.) for partial support. We thank the anonymous referee for useful comments that led to several improvements of the manuscript.

REFERENCES

Burrows, A., Livne, E., Dessart, L., Ott, C. D., & Murphy, J. 2007, ApJ, 655, 416
Campana, S., et al. 2006, Nature, 442, 1008
Chevalier, R. A. 1992, ApJ, 394, 599
Chevalier, R. A., & Li, Z.-Y. 1999, ApJ, 520, L29
Colgate, S. A. 1974, ApJ, 187, 333
Dai, Z. G., Zhang, B., & Liang, E. W. 2006, preprint (astro-ph/0604510)
De Luca, A. 2006, GCN Circ. 4853, http://gcn.gsfc.nasa.gov/gcn/gcn3/4853.gcn3
Ensman, L., & Burrows, A. 1992, ApJ, 393, 742
Fan, Y.-Z., Piran, T., & Xu, D. 2006a, preprint (astro-ph/0604016v1)
———. 2006b, J. Cosmol. Astropart. Phys., 9, 13
Ghisellini, G., Ghirlanda, G., & Tavecchio, F. 2007, MNRAS, 375, L36
Gorosabel, J., et al. 2006, A&A, 459, L33
Hamann, W. R., & Koesterke, L. 1998, A&A, 333, 251
Klein, R. I., & Chevalier, R. A. 1978, ApJ, 223, L109
Kulkarni, S. R., et al. 1998, Nature, 395, 663
Li, L.-X. 2007, MNRAS, 375, 240
Liang, E., Zhang, B., Zhang, B.-B., & Dai, Z. G. 2006, preprint (astro-ph/0606565)
MacFadyen, A. L., & Woosley, S. E. 1999, ApJ, 524, 262
Matzner, C. D., & McKee, C. F. 1999, ApJ, 510, 379
Mazzali, P. A., et al. 2006, Nature, 442, 1018
Meynet, G., & Maeder, A. 2007, A&A, 464, L11
Nugis, T., & Lamers, H. J. G. L. M. 2002, A&A, 389, 162
Schaerer, D., & Maeder, A. 1992, A&A, 263, 129
Soderberg, A. M., et al. 2006, Nature, 442, 1014
Tan, J. C. Matzner, C. D., & McKee, C. F. 2001, ApJ, 551, 946
Wang, X.-Y., Li, Z., Waxman, E., & Mészáros, P. 2007, ApJ, 664, 1026
Waxman, E. 2004a, ApJ, 602, 886
———. 2004b, ApJ, 605, L97
Waxman, E., & Loeb, A. 1999, ApJ, 515, 721
———. 2001, Phys. Rev. Lett., 87, 071101
Woosley, S. E., & Weaver, T. A. 1986, ARA&A, 24, 205